Nonlinear energetic particle modes: from bump-on-tail to tokamak plasmas

Matthew Lilley[1,4] B. N. Breizman[2], S. E. Sharapov[3], S. D. Pinches[3]

[1]Physics Department, Imperial College, London, SW7 2AZ, UK,
[2]Institute for Fusion Studies, The University of Texas at Austin, Texas 78712, USA
[3]EURATOM/CCFE Fusion Association, Culham Science Centre, Abingdon, OX14 3DB, UK
[4]Department of Earth and Space Sciences, Chalmers University of Technology, 41296 Göteborg, Sweden

Abstract

Energetic particle modes are often observed in present-day fusion experiments and they are of major importance for the next step burning plasmas. These instabilities exhibit a variety of nonlinear scenarios, from a steady-state saturated amplitude and frequency, to bursting amplitude evolution followed by significant frequency sweeping. Knowing the character of this nonlinear evolution is essential for understanding the global transport of the energetic particles and hence particle re-distribution and losses. The aim of the present talk is to demonstrate that, in spite of the significant differences in the nature of the modes, the nonlinear evolution, when driven just above their excitation threshold, is determined by a universal mechanism: the competition between the field of the modes and the relaxation processes that restore the unstable fast particle distribution function. In particular, we validate the recent theoretical finding that dynamical friction (drag) encourages beam-driven waves near marginal stability to exhibit an explosive scenario leading to frequency chirping (unlike velocity space diffusion). An efficient fully nonlinear numerical tool has been created for this task, using a bump-on-tail model. The results show characteristic features typical of any near threshold energetic particle driven instability, an example of which is asymmetric and hooked frequency sweeping modes. This work has galvanised the effort to perform dedicated experiments and quantitative modelling of the famous "chirping" modes in tokamaks by adding the collision operator to the HAGIS code. Results agree with the main trends of the bump-on-tail analysis.

Universal experimental signatures

Energetic particle driven Alfvénic instabilities are often observed in present-day fusion experiments and they are of major importance for the next step burning plasmas. These instabilities exhibit a variety of nonlinear scenarios for the mode amplitude and frequency evolution, from a steady-state saturated amplitude, to a bursting one. The nonlinear evolution, together with the linear stability criteria and the characteristic values of the amplitudes of the Alfvénic modes, are essential for understanding the global transport of the energetic particles and hence particle re-distribution and losses.

Experiments on Alfvénic instabilities driven by super-Alfvénic beams in the spherical tokamak MAST [1] exhibit a variety of modes excited in a broad range of frequencies from Alfvén Cascade (AC) eigenmodes (*FIG. 1*), Toroidal Alfvén Eigenmodes (TAE) (*FIG. 2*), and chirping modes in the frequency range 50-150 kHz, to compressional Alfvén eigenmodes (CAE) in the frequency range 0.4-3.8 MHz (*FIG. 3*), which is approaching the cyclotron frequency of plasma ions, $\omega \cong (0.1 \div 1)\omega_{ci}$. In spite of the differences in the nature of the modes (shear Alfvén or CAE), and in the corresponding excitation mechanisms, the nonlinear evolution of these modes, as seen in their spectrograms, show similarities.

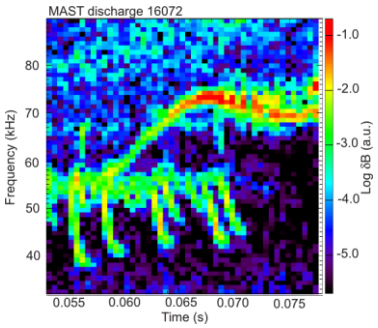

FIG. 1. Magnetic spectrogram showing AC and TAE

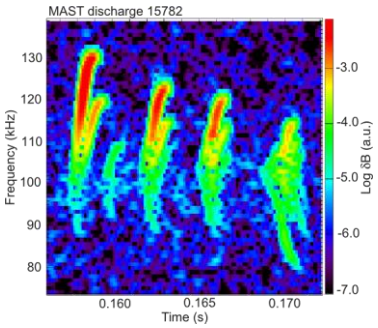

FIG. 2. Modes sweeping up in frequency over the TAE frequency range 90-130 kHz

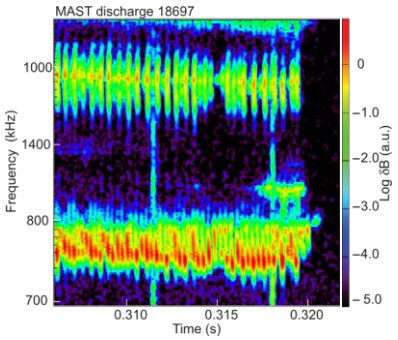

FIG. 3. Magnetic spectrogram showing bursting CAE (B=0.5 T, I=750 kA, P_{NBI}=3 MW)

This is consistent with the theoretical concept that, regardless of the specifics of the energetic particle driven instability, the nonlinear mode evolution just above the excitation threshold is determined by the competition between the wave field and the relaxation process restoring the unstable distribution function of the energetic particles. Moreover this competition reduces to a 1-D set of equations identical in form to that of the bump-on-tail problem [2]. It should be noted however that for high frequency modes, although the trends do appear to be the same as for low frequency modes, the theory has not been fully developed.

Modes driven by NBI vs those driven by ICRH

In MAST, the energetic particle population is created by super-Alfvénic neutral beam injection (NBI) with a maximum velocity V_{b0} satisfying $V_{b0} > V_A > V_{\mathrm{crit}}$. Here, V_A is Alfvén velocity, and V_{crit} is the critical speed at which the energy flow from energetic ions to thermal plasma electrons and ions becomes equal. Since the region of Cherenkov resonance, $V_{\|b} = V_A$, is well above V_{crit}, the Coulomb electron drag dominates over velocity space diffusion in the resonance region.

Experimentally, on MAST, as on some other machines with NBI, a 'hard' nonlinear regime is observed more often for NBI-driven Alfvénic modes, especially at low frequencies (e.g *FIG. 4*), resulting in bursting amplitude evolution and in rapid frequency sweeping [3-7]. Spontaneous formation of phase space holes and clumps [8] is typical of these NBI-driven scenarios [3]. The holes and clumps in the energetic particle distribution function correspond to resonant particles that are trapped in the field of the wave. These nonlinear structures can be viewed as long living Bernstein-Greene-Kruskal (BGK) modes [9], whose associated frequency can deviate far away from the original linear eigenfrequency. The theory was recently extended to include the case when the range of frequency sweeping is comparable to the frequency itself [10].

In contrast, Alfvén eigenmodes (AEs) excited by ICRH (ion cyclotron resonance heating)-produced ions show usually the 'soft' excitation regimes [11-16] (e.g *FIG. 5*). In these nonlinear scenarios, the mode frequency remains close to the linear AE eigenfrequency and the structure of the mode remains similar to the linear one.

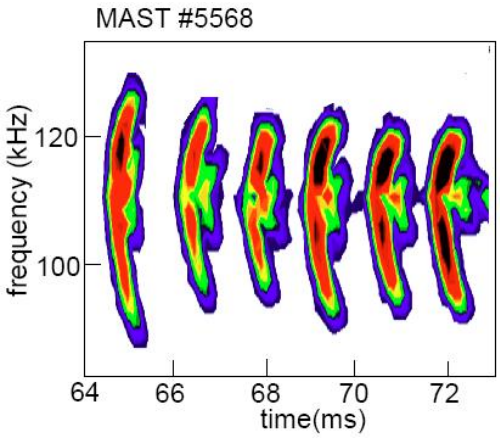

FIG. 4. Magnetic spectrogram of a MAST experiment with constant NBI power, showing rapid frequency sweeping

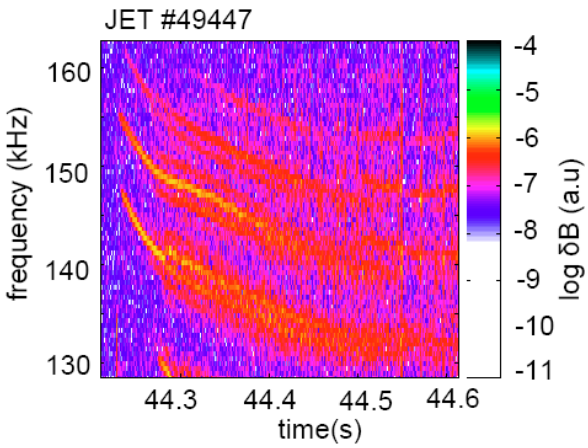

FIG. 5. Magnetic spectrogram of a JET experiment with slowly increasing ICRH power, showing a variety of soft non-linear regimes

The disparity between experiments on AE excitation by NBI and by ICHR has recently been attributed to the role of dynamical friction (drag) as a relaxation process for resonant particles [17]. This observation was made in the bump-on-tail model for a near threshold instability with $|\gamma_L - \gamma_d| << \gamma_d \leq \gamma_L$ where γ_L is the energetic particle contribution to the wave growth rate and γ_d is the wave damping rate due to dissipation in the bulk plasma. In the past such a model was successfully used to explain nonlinear bifurcations and frequency sweeping events observed in various AE experiments [3,11,12].

Dynamical friction

For energetic ions produced via neutral beam injection (NBI), the unstable distribution function is formed by Coulomb collisions, with dynamical friction (drag) and velocity space diffusion dominating in different regions of phase space. In contrast the relaxation processes for ICRH are dominated by velocity space diffusion due to the ICRH wave field. In the bump-on-tail problem with an unstable wave with wave number k and linear eigenfrequency ω_{pe}, the collision operator surrounding the wave particle resonance can be represented as

$$\left.\frac{dF}{dt}\right|_{\text{coll}} = \nu^3 \frac{\partial^2}{\partial u^2}\left(F - F_0\right) + \alpha^2 \frac{\partial}{\partial u}\left(F - F_0\right) \qquad (1)$$

where F is the distribution function of resonant fast particles, F_0 is the equilibrium distribution function, $u \equiv k\text{v} - \omega_{pe}$, and α and ν are constants characterising the dynamical friction and velocity space diffusion respectively. It was found [17] that the mode exhibits no steady state (see *FIG. 6*) and in fact grows explosively when dynamical friction (drag) dominates over velocity space diffusion in the vicinity of the wave-particle resonance, indicating the onset of chirping.

Translating the bump-on-tail results to beam driven TAEs reveals the ratio of diffusion to drag to be [17]

$$\frac{\nu_{TAE}}{\alpha_{TAE}} \approx mS\tau \frac{c}{eB_0}\frac{E_A}{r^2}\frac{\theta_b^4}{2}\frac{27}{64}\left(\frac{\pi m_b}{m_e}\right)^{3/2}\left(\frac{T_e}{E_A}\right)^{9/2} \quad (2)$$

Where m is the poloidal mode number (of order unity), m_b is the mass of the beam species, r is the minor radius, B_0 and T_e are the magnetic field and the electron temperature, E_A is the resonant Alfvénic energy, θ_b is the beam angle to the magnetic field, S is the magnetic shear, $\tau \equiv E_A^{3/2} m_b^{1/2} / \pi Z_b^2 e^4 n_e \ln\Lambda\sqrt{2}$. For MAST conditions we find

$$\frac{\nu_{TAE}}{\alpha_{TAE}} \approx 0.2 - 1.6 \quad (3)$$

showing that drag can be dominant in experiments, suggesting that drag could be responsible for the bursting behaviour of the TAEs on MAST. The same analysis for ITER parameters with alpha particles gives

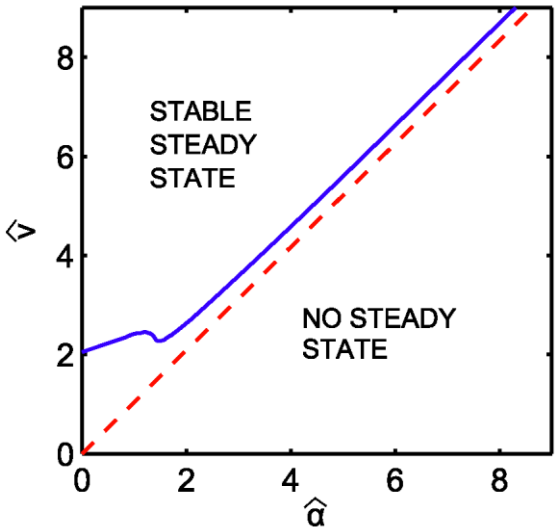

FIG. 6. Demonstrates that drag dominated regimes exhibit no steady state. Numerical simulations exhibits explosive behaviour in this case.

$$\frac{\nu_{TAE}}{\alpha_{TAE}} \approx 1.4 \quad (4)$$

showing that, although drag should not dominate, its effects should certainly be taken into account.

Fully nonlinear effect of dynamical friction

The previous analysis was limited to a weakly nonlinear regime with a perturbative treatment of the energetic particle response to the wave field. An extension to the analysis of [17], to describe the full nonlinear behaviour in drag dominated scenarios, has now been performed [18] and is largely based on numerical modelling using the BOT tool, which generalises an earlier code [19] to include the effect of drag.

We observe that the drag continues to play a destabilising role in the fully nonlinear problem [18]. It gives rise to the generation of holes and clumps (shown schematically in *FIG. 7*) in the fast ion distribution function, whose associated frequencies chirp asymmetrically from the original linear eigenfrequency as can be seen in *FIG. 8*. The drag enhances a phase space hole and acts to weaken, or even suppress, a phase space clump. The universal feature of all simulations including drag is the aforementioned asymmetry, which is also seen in experiments.

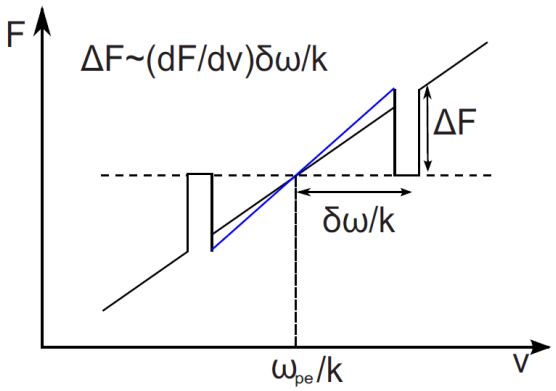

FIG. 7. Cartoon illustrating the initial motion of holes and clumps and the wake (blue line) that acts to steepen the distribution function, creating a favourable environment for instability.

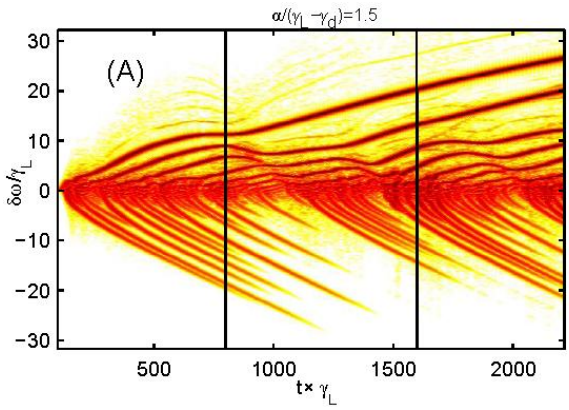

FIG. 8. Pure drag shows indefinite upward chirping holes and suppressed downward chirping clumps. Spectrogram shows the electric field increases indefinitely in time for the holes

The drag collision operator consists of two pieces, the first is a so called 'dynamic' part ($\partial F / \partial u$) that enters the kinetic equation formally in the same way as a DC electric field and the second is a so called 'sink' of particles ($\partial F_0 / \partial u$) that allows the formation of a steady-state solution of the unperturbed distribution function. The dynamic part provides energy to the wave in the form of fresh particles from high velocity. This is similar to the effect of chirping of holes and clumps. Both processes allow the wave to be sustained in the presence of background dissipation. The sink part acts to continually deepen a phase space hole, which prevents a steady state from forming.

Drag and diffusion

In reality, a system will exhibit both drag and diffusion. The effect of diffusion, unlike drag, is always to act to destroy a hole and a clump by filling the hole and depleting the clump. We observe [18] that a steady hole can be established when both drag and diffusion are present, as can be seen in *FIG. 9*. With somewhat more diffusion the steady state is lost and there is a tendency for the frequency and the electric field to undulate. With a further increase in diffusion the frequency spectrum exhibits intermittent hooks (*FIG. 10*). It is noteworthy that these hooks resemble experimentally observed chirping patterns [20].

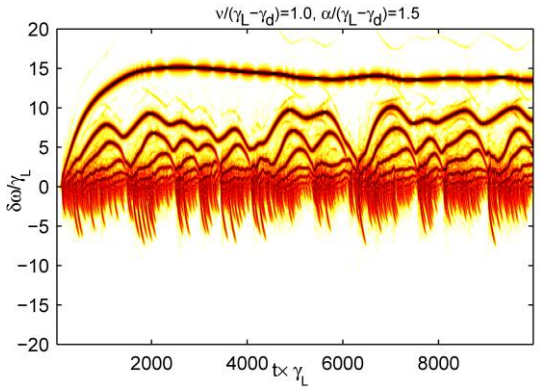

FIG. 9. Establishment of a steady state hole in the presence of both drag and diffusion

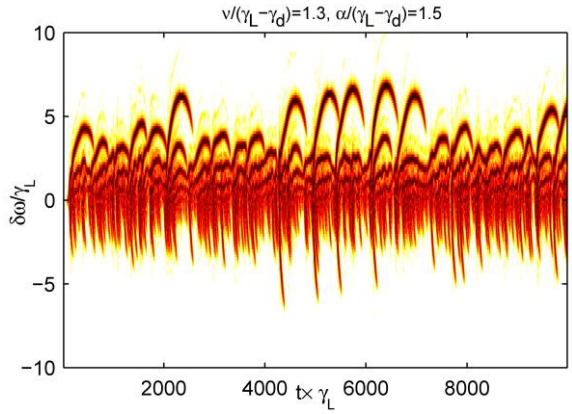

FIG. 10. Hooked frequency spectrum with drag and an increase in diffusion from that in Fig 9

These behaviours can be understood by recognising the competition that now exists between the sink in the drag collision operator that acts to deepen the hole, and the diffusion that acts to fill the hole. This competition can be captured using a simplified model that treats the wave as an ideal BGK mode [18]. More specifically the amplitude of a BGK wave defines a so called separatrix in phase space (of characteristic width ω_B / k where $\omega_B = \sqrt{ekE/m}$ is the bounce frequency for the particles trapped in the wave field) inside of which particles are trapped and mixed by the potential of the wave. It is these particles that form either a hole or a clump. For a wave whose frequency remains close to the plasma frequency one can write the wave equation in the form [18]

$$\delta\omega\omega_B = \frac{16}{3\pi^2}\gamma_L g \tag{5}$$

where, $\delta\omega$ is the frequency deviation and g is a measure of the relative depth of a hole to the ambient distribution, defined by $\Delta F = \left(\partial F_0 / \partial v\right) g / k$ (similar to that in *FIG.7*). For early times, or in the absence collisions $g = \delta\omega$, but in general we should write [18]

$$\frac{\partial g}{\partial t} + \left(\frac{48}{3\pi^2}\right)^{2/3} \frac{\nu^3}{1.84\omega_B^2} g = \frac{\partial \delta\omega}{\partial t} + \alpha^2 \tag{6}$$

so that the relative depth evolves in time due to the combined effect of drag, diffusion and chirping. Any flow of particles, either from drag or from the motion of the separatrix due to a changing wave frequency, cannot enter the separatrix and so make a jump to a lower velocity, which releases energy for a hole structure. By balancing the power released from drag and from chirping with the dissipation due to γ_d

$$\frac{3\pi^2}{48}\omega_B^3 = g\left(\frac{\partial \delta\omega}{\partial t} + \alpha^2\right) \tag{7}$$

(noting that it is assumed that the wave is driven close to the threshold so that $\gamma_d \approx \gamma_L$) a complete set of equations is formed allowing the frequency and electric field evolution to be calculated. Eqs (5) – (7) can be combined into a single parameter set of coupled nonlinear equations

$$\begin{aligned} x^2 &= y\left(\frac{\partial y}{\partial \tau} + 1\right) \\ a\frac{\partial (xy)}{\partial \tau} + \frac{y}{x} &= \left(1 + \frac{\partial y}{\partial \tau}\right) \end{aligned} \tag{8}$$

where $c\omega_B \equiv 1.84\alpha^4 x/\nu^3$, $\delta\omega \equiv \alpha^6 d 1.84^2 \gamma_L y/\nu^6$, $t \equiv \alpha^4 d\gamma_L \tau/\nu^6$, $a \equiv 1.84\alpha^4/\nu^3 d\gamma_L$ with $c \equiv \left(3\pi^2/48\right)^{1/3}$ and $d \equiv \left(3\pi^2/48\right)^{1/3}\left(16/3\pi^2\right)$. The behaviours in *FIGS.* 9 and 10 are reproduced by this reduced model, with the stability boundary of Eqs. (8) ($a = 1$) marking a dramatic change in behaviour from a steady state to one with hooked chirping. The full scale simulations agree with the trends of this model, namely parameters from Fig 8 give $a = 2.02$ (i.e. stable) whereas the parameters from *FIG. 9* give $a = 0.92$ (i.e. unstable). A numerical solution of Eqs (8) (shown in *FIG. 11*) for the unstable case reproduces the evolution of a single hook. The frequency and time scales are in good quantitative agreement with the well isolated hooks seen in *FIG.10* as shown in *FIG. 12*.

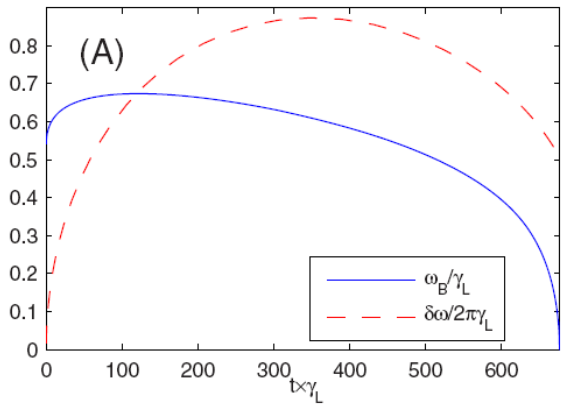

FIG. 11. Hooked chirp solution of Eqs 1.8, the solid line and dashed lines show the bounce frequency and the deviation of the frequency from the plasma frequency respectively.

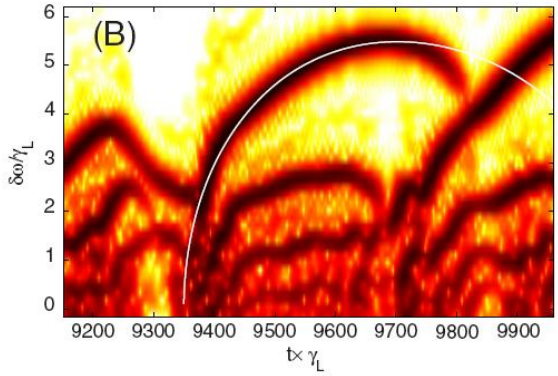

FIG. 12. Quantitative agreement between hooks seen in Fig 11 and Fig 12 (white line) is shown.

Drag in toroidal systems – HAGIS

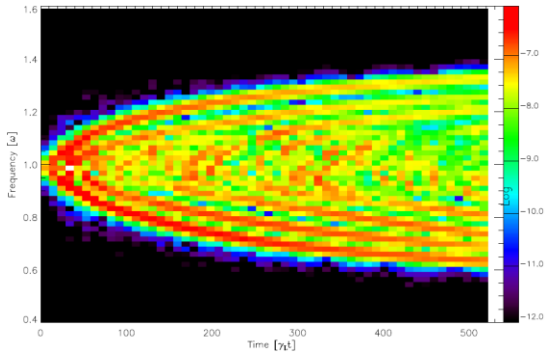

FIG. 13. Sliding Fourier transform showing frequency evolution of marginally unstable TAE mode in response to kinetic α-particle drive (γ_L/ω_0 = 0.0612) and external damping (γ_d/ω_0 = 0.06).

FIG. 14. This behaviour is very similar to that seen in the 1-D model introduced above and is more importantly, very similar to the mode evolution observed experimentally in e.g *FIG. 1.* This provides confidence in the use of simple models to investigate the nonlinear behaviour of modes near marginal stability and provides guidance on the physics aspects that need to be encapsulated in more sophisticated codes.

The effect of drag in realistic tokamak (i.e. toroidal) geometry has been investigated using a modified version of the HAGIS code [21] which includes the effect of drag and Krook relaxation upon the fast ions. *FIG. 13.* shows the results in the absence of drag for a core-localised n = 3 TAE interacting with a centrally peaked slowing-down distribution of α-particles which provide a linear growth rate of γ_L/ω_0 = 0.0612, in the presence of an extrinsic damping rate of γ_d/ω_0 = 0.06. Introducing an electron-ion drag of ν_{ei}/γ_d = 0.003 and a Krook relaxation rate of ν_{eff}/γ_d = 0.001 results in the spectrogram shown in

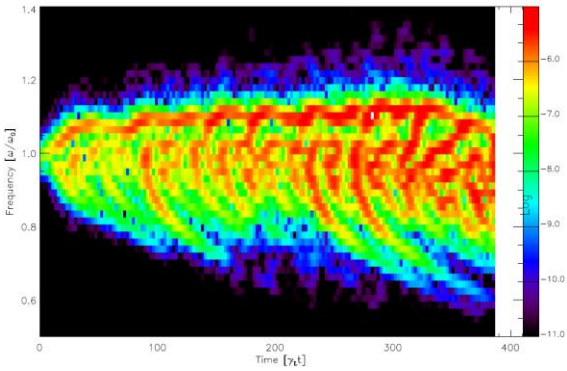

FIG. 14. Spectrogram showing influence of electron-ion drag and Krook relaxation upon mode evolution in tokamak geometry.

This work was funded jointly by the RCUK Energy Programme, the Swedish Research Council, EURATOM and by the U.S Department of Energy Contract No. DE-FG03-96ER-54326. The views and opinions expressed herein do not necessarily reflect those of the European Commission

References

[1] GRYAZNEVICH. M .P., SHARAPOV. S. E., et al., Nucl.Fusion **48** 084003 (2008)
[2] BREIZMAN. B. N., BERK. H. L., et al., Phys. Plasmas **4**, 1559 (1997)
[3] PINCHES. S. D., BERK. H. L., et al., Plasma Phys. Controlled Fusion **46**, S47 (2004)
[4] FREDRICKSON. E. D., GORELENKOV. N. N., et al., Nucl. Fusion **46**, S926 (2006).
[5] WONG. K. L., FONCK. R. J., et al.,Phys. Rev. Lett. **66**, 1874 (1991)
[6] HEIDBRINK. W., STRAIT. E., et al., Nucl. Fusion **31**, 1635 (1991)
[7] SHINOHARA. K., KUSAMA. Y., et al., Nucl. Fusion **41**, 603 (2001)
[8] BERK. H. L., BREIZMAN. B. N., Phys. Lett. A **234**, 213 (1997)
[9] BERNSTEIN. I. B., GREENE. J. M., Phys. Rev. **108**, 546 (1957).
[10] BREIZMAN. B. N., Nuclear Fusion **50**, 084014 (2010).
[11] FASOLI, A., BREIZMAN. B. N., et al., Phys. Rev. Lett. **81**, 5564 (1998)
[12] HEETER. R. F., FASOLI. A. F., Phys. Rev. Lett. **85**, 3177 (2000)
[13] WONG. K. L., WILSON. J. R., et al., Plasma Phys. Controlled Fusion **36**, 879 (1994)
[14] SAIGUSA. M., KIMURA. H., et al., Plasma Phys. Controlled Fusion **37**, 295 (1995)
[15] BERNABEI. S., BUDNY. R. V., et al., Nucl. Fusion **41**, 513 (2001)
[16] SNIPES. J. A., BASSE. N., et al., Phys. Plasmas **12**, 056102 (2005)
[17] LILLEY. M. K., BREIZMAN. B. N., et al., Phys. Rev. Lett. **102**, 195003 (2009)
[18] LILLEY. M. K., BREIZMAN. B. N., et al., Phys. Plasmas **17**, 092305 (2010)
[19] PETVIACHVILI. N., Ph.D. thesis, University of Texas at Austin, 1999.
[20] BERK. H. L., BOSWELL. C., et al., Nucl. Fusion **46**, S888 (2006)
[21] PINCHES. S. D. *et al.*, Comp. Phys. Comm. **111** (1998) 133
[22] LILLEY. M. K., Ph.D. thesis, Imperial College London, 2009.